

# Modeling fluid instabilities in inertial confinement fusion hydrodynamics codes\*

Steven T. Zalesak, Andrew J. Schmitt, and A. L. Velikovich  
*Plasma Physics Division, Naval Research Laboratory, Washington, D.C. 20375*

J. H. Gardner

*Laboratory for Computational Physics and Fluid Dynamics, Naval Research Laboratory, Washington, D.C. 20375*

The numerical tools typically used to model the evolution of fluid instabilities in inertial confinement fusion (ICF) hydrodynamics codes are examined, and some are found to have properties which would seem to be incompatible with the accurate modeling of small-amplitude perturbations, i.e., perturbations in the linear stage of evolution. In particular a “differentiability condition” which is satisfied by the physics in such situations is not necessarily satisfied by the numerical algorithms in typical use. It is demonstrated that it is possible to remove much of the non-differentiability in many cases, and that substantial improvement in one’s ability to accurately model the evolution of small amplitude perturbations can result. First a simple example involving a non-differentiable radiation transport algorithm is shown, and then the non-differentiabilities introduced by the use of upwind and “high resolution” hydrodynamics algorithms are analyzed.

## I. INTRODUCTION: NUMERICALLY MODELING THE EVOLUTION OF SMALL AMPLITUDE PERTURBATIONS

In Fig. 1 we show a schematic diagram of the problem which motivates this paper. We seek to numerically model the laser-driven implosion of a nearly spherically symmetric layered target in such a way as to effect the thermonuclear burn of its fusible components. In particular, we wish to be able to model the evolution of perturbations away from spherical symmetry with sufficient accuracy to be able to reliably compute the expected energy gain of the pellet. These perturbations, which can grow via Rayleigh-Taylor, Richtmyer-Meshkov, and other fluid instabilities, can originate in the initial conditions of the pellet, or be impressed upon the pellet by inhomogeneities in the laser radiation field. If they are small enough, they will initially undergo a period of linear evolution. If they are large enough, they may eventually transition to a more and more nonlinear regime, perhaps culminating in driven, fully turbulent flow. We are interested here in the accurate modeling of the early, linear, stages of perturbation evolution, for this evolution forms the critical initial conditions inherited by the nonlinear regime.

Although the inertial confinement fusion (ICF) pellet implosion motivates our discussion, we are actually interested in a much more general question: What are the appropriate numerical tools to accurately model the evolution of small-amplitude perturbations, when the unperturbed state itself may be time-dependent, highly nonlinear, and may contain spatial and temporal scales that are smaller than we can actually resolve, e.g., shock waves?

It is important to note that in the discussion throughout this paper we are assuming that all of the physical features of interest are smooth on some spatial and temporal scales, albeit scales that may be smaller than we can afford to actually resolve numerically. Thus when we pose questions of the physics, we assume differentiability at some finite scale ev-

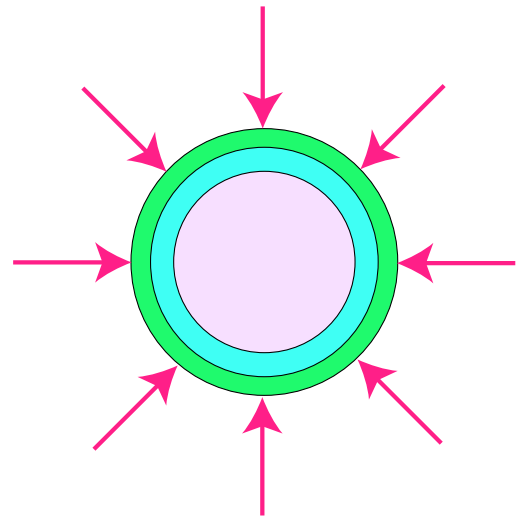


FIG. 1: Geometry of a laser-driven inertial confinement fusion (ICF) pellet. We are interested in accurately modeling the evolution of perturbations to this nominally spherically-symmetric configuration.

erywhere, but when we pose numerical questions, we do not necessarily assume that all such scales can be resolved on any mesh that we can afford to use. Even if we are treating interfaces between materials, we are assuming either that there is smoothness at some very small scale, or, equivalently, that the imposition of smoothness on some small scale will not affect the answers to any questions in which we have interest.

Since the above assumption of smoothness at some finite scale may cause some readers to pause, let us examine the reasons that we make such an assumption here, as well as the plausibility of the assumption. The reader will see below that we predicate our analysis on the linear behavior of additive infinitesimal perturbations, both in the initial conditions and in the subsequent evolution of the system. But a system that contains interfaces, i.e., true discontinuities in the state variables, either in the initial conditions or in its subsequent evolution, simply cannot be described in terms of ad-

---

\*This work was supported by the U.S. Department of Energy, NNSA.

ditive perturbations unless one is using a coordinate system that is moving with the interfaces, e.g., a Lagrangian coordinate system in the case of material interfaces. Thus it could be argued that the analysis we present below is not applicable to such situations unless one is using such a coordinate system. Nonetheless we believe strongly that the analysis we present below is applicable. Our reasons are two. First, there are physical dissipative processes active in all plasmas which prevent the maintenance of discontinuities in state variables, e.g., mass diffusion, viscosity, and conductivity. The scale sizes produced by these mechanisms may be smaller than can be resolved numerically, in which case a numerical simulation that included these mechanisms would be virtually identical to one which did not, but the physical scale sizes are finite nonetheless, thus making our assumptions valid. Second, the interface instabilities in which we are interested in general do not have their behavior significantly changed if we approximate them as narrow but smooth transitions between two states. This is explicitly acknowledged in the formulae we use to approximate the growth rate of the ablative Rayleigh-Taylor instability, for example, wherein a factor  $(1 + kL)^{-1}$  pre-multiplies the Rayleigh-Taylor interface growth rate term to allow for finite plasma gradient scale length effects, where  $k$  is the transverse Fourier wave number of the perturbation and  $L$  is the gradient scale length ([1], pg. 62). Clearly a sufficiently small but finite  $L$  has a negligible effect on the interface growth rate in this instance. Another example is the fact that accounting for physical viscosity and heat conduction in the compressible fluid equations near a shock wave broadens the shock front, but does not change the shock's propagation speed or the jumps across the shock front. (This is even true numerically as well as physically if we use numerical methods which conserve mass, momentum and total energy at the discrete level, as we do here.) Nonetheless, the reader should be cognizant of the fact the the arguments we present below cannot be rigorously shown to be applicable to situations in which true discontinuities exist.

## II. THE LINEAR EVOLUTION OF INFINITESIMAL PERTURBATIONS: THE DIFFERENTIABILITY CONDITION

We will frame our discussion within that of systems of conservation laws, which take the form

$$\frac{\partial q_i(\mathbf{x}, t)}{\partial t} + \nabla \cdot \mathbf{f}_i(q_1, q_2, \dots, q_m, \mathbf{x}, t) = 0; \quad i = 1, m \quad (1)$$

where  $\mathbf{x}$  and  $t$  are space and time respectively, and  $m$  is the number of conservation laws in the system. Examples of such equations include the Navier-Stokes equations, the equations of magnetohydrodynamics (MHD), the Vlasov equation, passively-driven convection, and, of course, our ICF pellet implosion scenario.

As we have stated before, we shall assume that the initial conditions  $q(\mathbf{x}, 0)$  are smooth at some sufficiently small spatial scale, and that there is present in the physics some dissipative mechanism active at some finite but perhaps small spatial

and temporal scales to ensure that the solution  $q(\mathbf{x}, t)$  is also smooth at those scales. We do not, however, assume that we can actually resolve all such scales numerically.

The above notwithstanding, we will try to impose on our numerical algorithms the following property of the physics: If we confine our perturbation to that of the initial condition  $t = 0$ , then in the limit of vanishing perturbation amplitudes about virtually any unperturbed time-evolving system, there exists a constant of proportionality between any component of the initial perturbation and any other component of the evolved perturbation at some fixed later time. This constant of proportionality is precisely the partial derivative of the latter with respect to the former.

In particular the following ‘‘linearity’’ property holds: We define a physical time evolution operator  $T$  which advances the physical solution in time from  $t = 0$  to  $t = t_f$ :

$$q(t_f) = T(q(0)) \quad (2)$$

where we have dropped the notational dependence of  $q$  on  $\mathbf{x}$  for clarity. We do the same for the perturbation quantities  $p_1$  and  $p_2$  below.

For the laser-driven ICF problem of interest here,  $T$  is a nonlinear *differentiable* operator on  $q$ , i.e.,  $q(t_f)$  is a differentiable function of  $q(0)$ , unless we find ourselves at a bifurcation point in chaotic flow. For the purposes of this paper we assume that we are not at such a bifurcation point.

We now introduce infinitesimal perturbations  $p_1(\mathbf{x})$  and  $p_2(\mathbf{x})$  to the initial conditions. From the differentiability of  $T$  and the assumption that  $p_1(\mathbf{x})$  and  $p_2(\mathbf{x})$  are infinitesimal it follows that in the limit of vanishing perturbation amplitudes:

$$T(q + \alpha p_1) - T(q) = \alpha(T(q + p_1) - T(q)) \quad (3)$$

where  $\alpha$  is a scalar, and

$$T(q + p_1 + p_2) - T(q) = T(q + p_1) + T(q + p_2) - 2T(q) \quad (4)$$

where we have dropped the notational dependence of  $p_1$  and  $p_2$  on  $\mathbf{x}$  for clarity.

Equations (3) and (4) above define a perturbation evolution that is normally described as ‘‘linear.’’ They apply whether the growth or decay of the perturbation is exponential in time, as it is for the Rayleigh-Taylor instability, or has some other time dependence, as is the case for the Richtmyer-Meshkov instability. The terminology aside, they describe the *physical* behavior of infinitesimal perturbations to the basic flow defined by  $T(q)$ . It is the primary thesis of this paper that a necessary, or at least highly desirable, condition for the successful numerical modeling of the evolution of extremely small perturbations to a specified physics problem, like that of the imploding ICF pellet, is that the numerical time evolution operator  $T_n$  satisfy the very same equations. Henceforth, when a given numerical time evolution operator  $T_n$  satisfies equations (3) and (4), we shall say that that  $T_n$  satisfies the ‘‘differentiability condition.’’ Surprisingly perhaps, many of the numerical methods in use in modern ICF codes fail this test.

### III. NON-DIFFERENTIABLE ALGORITHMS IN MODERN ICF CODES

In the last section we put forth the thesis that a numerical time evolution operator  $T_n$  should satisfy the differentiability condition, i.e., satisfy equations (3) and (4), if we wish to accurately model the evolution of small perturbations to a physical system. A legitimate question for anyone not fully familiar with ICF codes might be the following: How could such non-differentiability possibly find its way into such codes? Looking at Eq. (1), we see that our numerical task is simply to perform discretizations of spatial and temporal derivatives. Certainly the obvious finite difference and finite element formulations of such derivatives do not introduce any non-differentiability, so barring any inherent non-differentiability in the equations themselves, where could such non-differentiability possibly originate? Rather than attempting to answer this question comprehensively, let us simply list some of the places where one might find a lack of differentiability in such codes:

1. “High resolution” numerical algorithms for fluid dynamics, sometimes known as “modern front-capturing methods” or “modern shock-capturing methods.”
2. Upwind methods for fluid dynamics (at sonic points)
3. “Sharp cutoff” flux limiters for thermal conductivity, and for radiation diffusion
4. Linear interpolation in table lookups for equation of state data and opacities

The non-differentiability associated with the last item above will hopefully be obvious to the reader, as will the fact that creating a table lookup interpolation procedure with continuous derivatives, that also avoids the possibility of spurious interpolated values, may be a challenging problem for some data sets. The remaining three items will be explored in the following sections.

#### A. Symptoms of Numerical Non-differentiability

An infinitesimally perturbed solution that encounters a point of non-differentiability will exhibit a false nonlinear response of some kind. A pure Fourier mode in a periodic problem may not remain pure, for example. This can only happen if the numerical algorithm used has points of non-differentiability inside an “envelope” of the solution space spanned by the unperturbed solution on the one hand and by its perturbed counterpart on the other. In that case, the perturbed solution must at some point in its history have “crossed” a point of non-differentiability, perhaps many times if the perturbation is oscillatory in space or time, seeing one derivative on one side of the crossing point, and another on the other. Clearly as the amplitude of the perturbation becomes smaller and smaller, the envelope in solution space in which the point of non-differentiability must reside becomes smaller

and smaller. Thus, unless a point of non-differentiability resides directly on the unperturbed solution, one can easily become just plain “lucky” in any given calculation, with no symptoms at all, and yet encounter a major “glitch” with the same numerical software on a modestly different problem. We will see an example of this in a later section. On the other hand, even if a point of non-differentiability is encountered, the result may or may not be harmful, or even measurable. This will clearly depend on many factors, including the size and location of the point of non-differentiability.

Thus, by simply running computational examples with various algorithms, as we do here, it will be impossible to prove that the reason an algorithm failed is that it was non-differentiable, or that the reason another succeeded was that it was differentiable. All we can do here is try to lend some empirical plausibility to our hopefully plausible hypothesis. Our task is made all the more difficult by the fact that it is probably impractical to construct real ICF codes with algorithms that are completely differentiable over all of solution space.

#### B. An Example of the Effects of Numerical Non-differentiability

As we have stated previously, one of the possible sources of non-differentiability in ICF codes is the use of sharp cut-off radiation diffusion and thermal conductivity flux limiters. We refer the reader to ([2], pp 478-481) for the motivation and form of such flux limiters in the radiation diffusion case, the case we shall examine in this section. Briefly, the diffusion approximation used in many ICF codes can produce fluxes of radiant energy  $F(s)$  that exceed what is physically possible  $F^{max}(s)$ . Here  $s$  represents all of the parameters on which  $F$  may depend, e.g., the local radiation energy density gradient and Rosseland mean opacity. In that case, one of the remedies is to limit the flux  $F(s)$  so that it does not exceed  $F^{max}(s)$ . The obvious “sharp cut-off” solution is simply

$$F(s) = \min(F(s), F^{max}(s)) \quad (5)$$

Clearly Eq.(5) defines a flux which is a non-differentiable function of its arguments at all values of  $s$  for which  $F(s) = F^{max}(s)$ . An alternative flux limiter is the so-called “harmonic mean” limiter:

$$F(s) = F(s)/(1 + F(s)/F^{max}(s)) \quad (6)$$

which is a differentiable function of its arguments. These are the two flux limiters that we examine below.

In Figures 2 and 3, we show the results of a pair of 2D  $r - \theta$  laser pellet implosion simulations using the Naval Research Laboratory’s (NRL’s) FAST code [3]. The pellet and imposed laser intensity profile are described in [4]. Briefly, the pellet is a pure deuterium-tritium (DT) shell of outer radius 0.169 cm and thickness 0.034 cm, driven by 0.351  $\mu\text{m}$  wavelength laser radiation at an intensity of 10 TW for the first 4 nsec, and ramping monotonically to 450 TW at 6.05

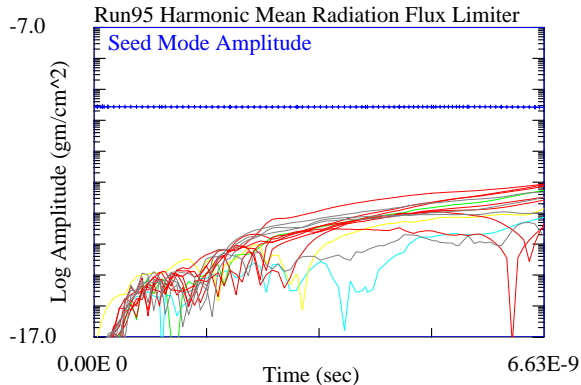


FIG. 2: Legendre mode amplitude of areal mass density vs. time for a FAST run of a NIF pellet using an extremely small Legendre  $l = 2$  perturbation, and using a harmonic mean (differentiable) radiation flux limiter. The Legendre spectrum should, and is, dominated by the nearly static seed perturbation during this early-time evolution. The seed mode is plotted as a thick line with embedded “+” symbols, while the other Legendre modes are plotted as simply thin lines

nsec, where it stays until laser turn-off at 8.6 nsec. A single  $l = 2$  Legendre mode perturbation of extremely small amplitude is imposed on the outer surface. The quantity of interest is the integrated (in  $r$ ) areal mass density as a function of  $\theta$ , here analyzed in Legendre space. We calculate only the very early time behavior here, terminating the simulation shortly after the first main shock has broken out through the interior surface of the pellet. The physics is such that one should see a nearly static evolution of the  $l = 2$  mode, with little or no generation of other Legendre modes during this early phase of the pellet implosion. In Fig. 2 we show Legendre mode amplitude vs. time for a calculation which used the harmonic mean radiation diffusion flux limiter Eq. (6), which is a differentiable function of its arguments. Note that the behavior of the Legendre modes is qualitatively what we expect: a nearly static seed mode, with small amplitudes maintained for all the other modes. In Fig. 3 we show the results for a simulation which was identical to that in Fig. 2, except that we are now using the sharp cut-off version of the radiation diffusion flux limiter Eq. (5), which is a *not* a differentiable function of its arguments. Note the dramatic difference in the results, with the unphysical generation of higher order harmonics which eventually drive even the primary  $l = 2$  mode away from its physically correct amplitude.

This one simple example makes it clear that non-differentiable numerical algorithms are a potential serious threat to the accuracy of simulations of small-amplitude perturbations on ICF laser pellets.

#### IV. UPWIND METHODS AND “HIGH RESOLUTION” METHODS AS SOURCES OF NON-DIFFERENTIABILITY

While we again wish to emphasize that any source of numerical non-differentiability should be viewed as a threat to

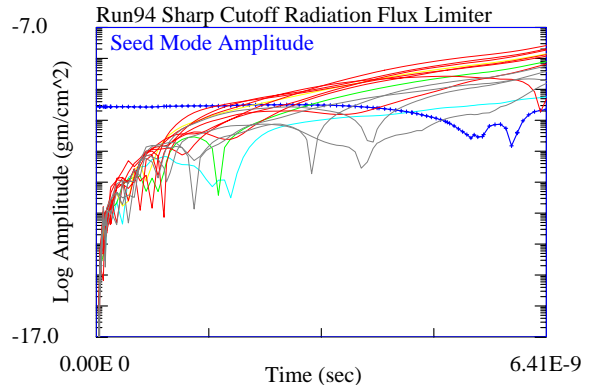


FIG. 3: Same as Fig. 2, but using a sharp cut-off (non-differentiable) radiation flux limiter. Note the quick non-physical rise of other Legendre modes, a numerical artifact caused by the use a non-differentiable numerical algorithm.

accuracy, we will for the remainder of this paper focus on hydrodynamics algorithms. Specifically, we will investigate the first two sources of non-differentiability from our list in the previous section: “high resolution” methods and upwind methods. The use of these methods as opposed to standard (differentiable) finite difference and finite element methods derives from the same need: the need to robustly deal with structures too small to be resolved on any reasonable spatial or temporal mesh, as we explore in the paragraphs that follow.

As we stated in our assumptions, as long as there is some dissipative mechanism active at some finite but perhaps small scales, solutions to (1) with smooth initial conditions will remain smooth for all time. However, in many such systems, including compressible fluid dynamics, the system can and often does evolve in such a way to produce small regions over which the solution or its derivatives can change dramatically. If these regions are smaller than a mesh size, from a numerical viewpoint we are treating discontinuities. We will term such unresolved regions “fronts” for the purpose of this paper. Given that we do not wish to actually resolve these fronts, we demand instead that they be represented numerically as narrow regions on our grid without numerical artifacts that contaminate adjacent regions, that they propagate with the correct speed, and that the jumps across them are physically correct. In most cases this situation is addressed by the Lax-Wendroff Theorem ([5]), which states that if one’s numerical approximation to Eq. (1) is in “flux” or “conservation” form, and the solution converges everywhere but on a set of measure zero to some solution, and in addition satisfies an entropy inequality, then the above demands will be met. Thus the great majority of methods designed to treat fronts in the context of Eq. (1) are in conservation form, i.e., a form consisting of numerical fluxes connecting adjacent grid points, these fluxes being used to advance the numerical solution in time.

Using conservation form does not by itself give the desired result however, since one still needs to compute a convergent solution. In general, numerical methods not designed to deal with fronts will not produce the desired convergence in their

presence, often producing numerical oscillations that degrade the solution severely. Most often, successful methods use some sort of explicit or implicit artificial numerical dissipation to achieve such convergence.

Over the past 30 years a host of algorithms, known variously as “modern front-capturing methods,” “modern shock-capturing methods,” or “high resolution methods,” have been developed in an attempt to perform calculations containing fronts more accurately and more efficiently than with the more traditional artificial dissipation approaches. The first of these methods was flux-corrected transport (FCT) [6, 7], but there are now a large number of others (e.g, MUSCL [8], PLM [9], PPM [10], ENO [11], WENO [12, 13], TVD [14] methods, and Discontinuous Galerkin (DG) methods [15]). What distinguishes the “high resolution” methods from their predecessors is their attempt to constrain the numerical fluxes, grid point by grid point and timestep by timestep, in such a way as to avoid the production of unphysical values in the solution vector  $\mathbf{q}$ .

A well-known theorem by Godunov [16] states that any linear algorithm that guarantees the avoidance of unphysical values renders the algorithm at most first order accurate in time and space. Thus all modern front-capturing algorithms of order greater than one must be inherently nonlinear operators. However, almost without exception, these modern front-capturing methods involve the use functions that are not just nonlinear, but *non-differentiable* as well, using  $\min$ ,  $\max$ ,  $\text{abs}$ , and  $\text{sign}$  operators, as well as similar functions involving *if-then-else* statements. Thus at a fundamental level, time evolution operators incorporating such algorithms are non-differentiable functions of their arguments. Compounding the above sources of non-differentiability is the fact that many of these algorithms use upwind algorithms, which have their own set of non-differentiabilities, as building blocks. In particular, the numerical fluxes associated with upwind methods are non-differentiable functions of the hydrodynamic wave speeds, at all points at which such wave speeds vanish in the frame of reference of the grid. (These are the places in the flow where  $u - c$ ,  $u$ , and  $u + c$  vanish, where  $c$  is the local sound speed and  $u$  is the local fluid speed. We shall use a loose definition here, and call all such points “sonic points.”) Thus the use of even simple first order upwind methods like Godunov’s method [16] would seem to be at odds with our desire to accurately model the evolution of small amplitude perturbations, with the “high resolution” methods being riskier still. Let us therefore perform some numerical experiments to see if we can determine just how risky some of these methods may be in the context of our laser pellet implosion problem.

The algorithms we choose for investigation, in order of increasing differentiability, are

- The Piecewise Linear Method (PLM) of Colella and Glaz [9] (non-differentiable whenever the slope limiter is active, and at all sonic points)
- The first-order Godunov method [16] (non-differentiable at all sonic points)
- A first order donor cell method plus a Richtmyer-Von

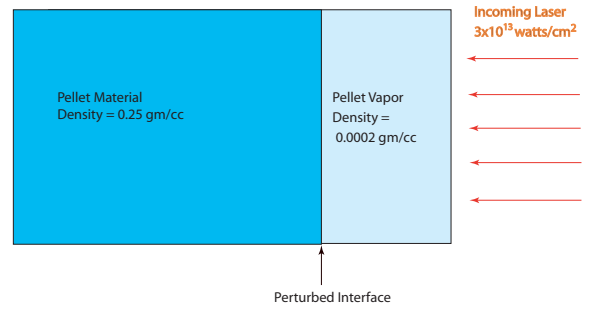


FIG. 4: Geometry of laser-driven pellet test problem.

Neumann artificial viscosity (non-differentiable only at entropy wave ( $u = 0$ ) sonic points)

- The Richtmyer two-step Lax-Wendroff algorithm ([17], pp. 302-303)(differentiable everywhere)

Note that only the Lax-Wendroff method is truly differentiable.

## V. A NUMERICAL TEST PROBLEM

We choose as our test case a simplified version of the early-time pellet implosion problem. As depicted in Fig. 4, a semi-infinite slab of a monatomic ideal gas at one atmosphere pressure and a density of  $0.25 \text{ g/cm}^3$  is irradiated uniformly from the right with 0.35 micron laser radiation, with an intensity of  $3 \times 10^{13} \text{ W/cm}^2$ , starting at  $t = 0$  and lasting indefinitely. A simple 2D code that we dubbed “Sandbox” was written which incorporated the three most critical physics modules, which were applied using operator splitting:

- Laser absorption via inverse Bremsstrahlung, using the prescription of Johnson and Dawson [18], modified to ensure differentiability.
- Spitzer-Harm thermal conductivity [19] without flux limiting (again to ensure differentiability)
- one-dimensional hydrodynamics algorithms applied to two dimensions using operator splitting

The two-dimensional calculation was then performed on a  $800 \times 16$  grid using grid spacings of 0.1 microns and 1.5 microns in the  $x$  and  $y$  directions respectively.

The interface between the pellet material and its vapor is placed at the midpoint in a cell, ensuring that for sufficiently small interface perturbations, the numerical perturbation will take the form of additive density perturbations to the numerical grid quantities. (Recall that our definition of differentiability is with reference to additive perturbations.) A sinusoidal perturbation of wavelength 24 microns is applied to the position of the interface, with an amplitude of 0.0005 microns. This amplitude is sufficiently small that physical nonlinear effects should be extremely small, and the response of the system to the perturbation should be linear to many orders of

magnitude. The physics is such that, after some initial transients, a quasi-steady ablation region approximately 1.7 microns wide establishes itself, propagating into the pellet material as ablated low density material is blown off toward the incoming laser. A strong shock propagates away from the ablation region into the pellet. Both the ablation region and, to a lesser extent, the shock are regions of strong perturbation evolution.

Analysis of this perturbation problem by Velikovich et al. [20] and by Goncharov et al. [21] reveals that the evolution can be described in terms of a quantity that can be measured experimentally, the integrated mass density  $M(y)$  along the laser path.  $M(y)$  starts and remains a constant plus a small sinusoid. Plotting the sinusoid's amplitude as a function of time reveals semi-periodic nulls at which phase reversal takes place. At any given moment in time during a calculation, we should be able to compute  $M(y)$ , and compute its Fourier transform. If our calculation is performing properly, we should see a DC component, and one other finite amplitude component at the seed mode wavelength. The amplitude of all other Fourier modes should be due solely to nonlinear coupling terms, second and higher order in the perturbation amplitude, and hence extremely small given the extremely small perturbation amplitudes we are using here. Thus in the following plots we use the following definitions:

- “Seed Amplitude” is simply the amplitude of the seed mode as given by the numerical Fourier transform of  $M(y)$ .
- “Noise” is the result of numerically removing from  $M(y)$  both the DC component and the seed mode, and taking the maximum absolute value of the remaining values. Note that this is an extremely sensitive measure of “noise.” In fact, sufficiently small levels of “noise” may in fact represent physically correct second and higher order nonlinear coupling terms, as we mention above.

## VI. NUMERICAL TESTS OF HYDRODYNAMICS ALGORITHMS IN 2D PLANAR GEOMETRY

The Sandbox code has been used to run many tests of numerical hydrodynamics algorithms. Here we have chosen just five of those calculations which illustrate the potential benefits of maximizing differentiability in such algorithms.

- Test 1: Godunov hydrodynamics used for both the  $x$  and  $y$  directions.
- Test 2: Godunov hydrodynamics used for both the  $x$  and  $y$  directions, with multidimensional Colella-Woodward-Lapidus artificial dissipation used in both directions (see discussion below)
- Test 3: Godunov hydrodynamics used for the  $x$  direction and Lax-Wendroff used for the  $y$  direction, with no additional artificial dissipation.

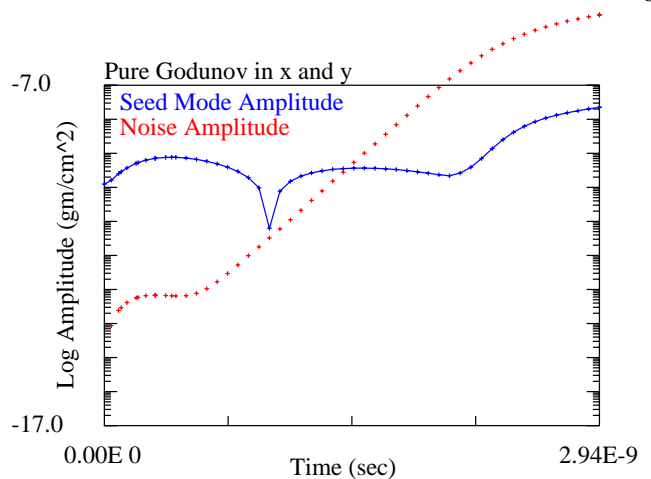


FIG. 5: Seed mode amplitude (line) and noise amplitude (“+” symbols) versus time for a simulation using the Godunov algorithm in both the  $x$  and  $y$  directions.

- Test 4: PLM used for both the  $x$  and  $y$  directions, with no additional artificial dissipation..
- Test 5: PLM used for the  $x$  direction and Lax-Wendroff used for the  $y$  direction, with no additional artificial dissipation.

**Test 1** In Fig. (5 we show the seed mode amplitude and noise amplitude versus time for Test 1. Although the seed mode behaves correctly (see below) for the first half of the simulation, its amplitude is thereafter exceeded by that of the noise, and it exhibits incorrect behavior after that point. Our diagnosis is that the Godunov’s non-differentiability at all sonic points gives rise to this false nonlinear behavior, making it an inappropriate choice for the accurate modeling of small amplitude perturbations for this problem.

**Test 2** If our diagnosis of the problems seen in Test 1 is correct, we need to eliminate some of regions of non-differentiability in our algorithms if we are to have any hope of solving our problem accurately. We will do that below, but first let us look at another possible diagnosis of the above problem: that we are witnessing the symptoms of the “carbuncle phenomenon” [10, 23] This term refers to the difficulty that upwind methods like the Godunov method have when dealing with perturbed shock waves traveling parallel or nearly parallel to one of the mesh lines of a grid, precisely the situation we have here. While the true causes of the phenomenon are still a subject of debate, the “cure” is nearly always to add an extra amount of artificial dissipation transverse to the shock propagation direction. Indeed, Colella and Woodward [10] suggest a multidimensional variant of Lapidus artificial dissipation which closely resembles most of the remedies suggested by more modern papers. Thus, in Fig. 6 we show the results of simply adding that dissipation to the algorithm used in Test 1. We see that the “carbuncle” hypothesis seems to be plausible: there are two clean phase reversals, and the seed mode amplitude is decreasing in time, in accordance

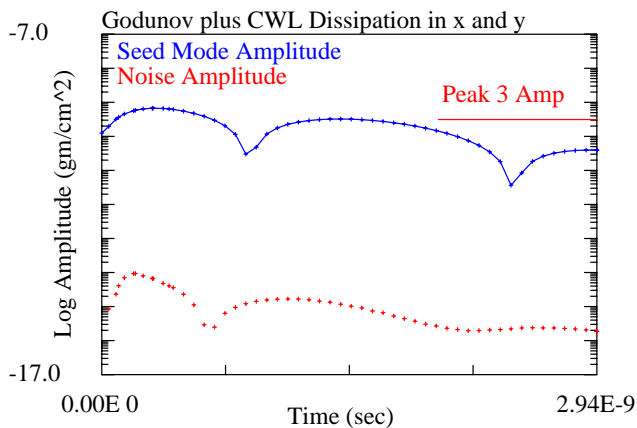


FIG. 6: Seed mode amplitude (line) versus time and noise amplitude (“+” symbols) versus time for a simulation using the Godunov algorithm in both the  $x$  and  $y$  directions. Extra Colella-Woodward-Lapidus artificial dissipation was added in both directions. The line labeled “Peak 3 Amp” indicates the expected value of the third temporal maximum in the seed mode amplitude, near 3 nsec, using the analytic techniques of [22]. Note that although our results show good clean linear evolution, with the expected two phase reversals in the time interval, we are nonetheless also showing considerable false numerical damping of the seed mode in time.

the the semi-analytic results of [22], which predicts a slow decay of the seed mode in time, with two phase reversals in the interval between 0 and 3.0 nsec. More importantly, except in the vicinity of the phase reversal points, our signal-to-noise ratio is roughly  $10^5$  to 1, indicating that our pure Fourier mode is remaining pure, i.e., that the code is responding in the differentiable/linear manner that it should. However, we also note in the figure that the simulation is predicting a damping of the seed mode amplitude in time that is considerably larger than we expect from the semi-analytic results. We return to this point later.

**Test 3** Instead of the “carbuncle” diagnosis of the problems encountered in Test 1, which dictates a “cure” of increased numerical dissipation, let us now pursue a solution based on our hypothesis of non-differentiability as the cause of Test 1’s difficulties: We know that the only non-differentiable points for the Godunov method are the sonic points, which exist in both the  $x$  and  $y$  directions. We also know that our perturbation is extremely small, meaning that the “envelope” in solution space in which our numerical solution will encounter problems will be correspondingly small, unless of course the unperturbed solution itself rests directly on one of the sonic points. A little reflection by the reader will hopefully convince him or her that in the  $x$  direction we would have to be quite unlucky for one of our numerical flux evaluation points to fall inside the envelope. But in the  $y$  direction, the unperturbed solution sits directly on the entropy wave sonic point, since for the unperturbed solution  $u_y = 0$  everywhere. Thus if our perturbed solution is oscillatory in space, which it is, we cannot escape being caught in the envelope every single timestep.

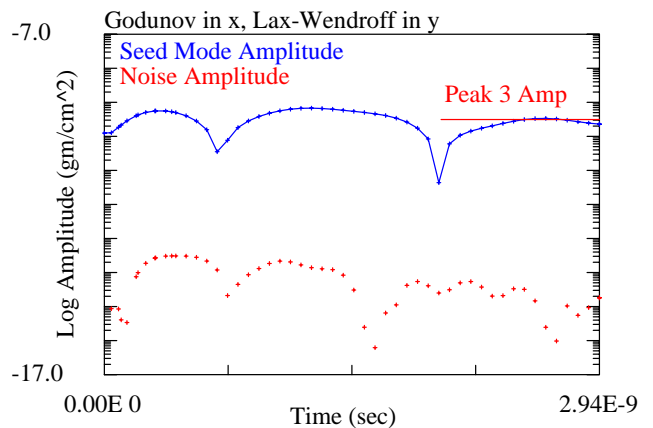


FIG. 7: Seed mode amplitude (line) versus time and noise amplitude (“+” symbols) versus time for a simulation using the Godunov algorithm in the  $x$  direction and the Lax-Wendroff method in the  $y$  direction. No extra artificial viscosity was added in either direction. The line labeled “Peak 3 Amp” indicates the expected value of the third temporal maximum in the seed mode amplitude, near 3 nsec, using the analytic techniques of [22]. Note that we have achieved the same clean results as in Test 2, and at the same time have been able to maintain the amplitude of the seed mode near the value given by theory.

This reasoning would suggest that we may be able to address Test 1’s problems by using a differentiable algorithm in the  $y$  direction. Since the solution is, for these early times, smooth in that direction, we can and do choose the fully differentiable Lax-Wendroff method. Note that we are suggesting a solution which is in exactly the opposite direction from that given by the usual “carbuncle” remedy: By changing from the Godunov method to the Lax-Wendroff method we are *removing* large amounts artificial dissipation rather than adding it. In Fig. (7) we show the results of that experiment. Note that the results are even better than those of Test 2. Not only are our signal-to-noise ratios roughly  $10^5$  to 1, but the seed mode amplitude near 3 nsec is much higher, in very close agreement to that given by theory.

We again point out that we have arrived at two totally disparate approaches to remedying the problems of the Godunov method in Test 1: 1) adding dissipation in the  $y$  direction; and 2) removing non-differentiability in the  $y$  direction, and in the process *removing* dissipation in the  $y$  direction. We hypothesize here that the first remedy is nothing more than a cosmetic fix, hiding the true cause of the “carbuncle” phenomenon under a mountain of numerical dissipation. Addressing the problem in terms of its true cause, i.e., failure to satisfy the differentiability condition, is by far the better approach, yielding a clean linear response without the side effects of large amounts of numerical dissipation.

**Tests 4 and 5** Although we do not include the figures here, we will describe the results. The reader may see that Tests 4 and 5 are merely the higher order variants of Tests 1 and 3 respectively. They yield similar results, with Test 4 showing

unacceptable growth of noise in the time interval 0 to 3 nsec, and Test 5, despite the added but improbably crossed non-differentiabilities added by the use of PLM in the x-direction, yielding good clean results, albeit with signal-to-noise ratios in the  $10^3$  to 1 range, as opposed to the  $10^5$  to 1 range of Test 3. Thus it would appear that even the more modern “high resolution” methods can sometimes be used, at least in circumstances where the risk incurred by their failure to satisfy the differentiability condition is small. The user of such methods must still be wary however, for they can and will occasionally trip over their own points of non-differentiability. We look forward to the future development of “high resolution” methods that are free of such points. Note that the development of “high resolution” methods satisfying the differentiability condition is not precluded by Godunov’s Theorem, since the theorem merely demands that such algorithms be nonlinear, not that they be non-differentiable.

We have also run similar tests in radial geometry, not shown here, wherein shocks can focus and reflect from the origin, and we find there an increase in sensitivity to non-differentiability. We have found at least one case where our perturbed solution crosses, albeit “unluckily,” a  $u + c$  sonic point in the radial direction, causing a catastrophic disruption of linearity at all subsequent times. However, if we simply reverse the sign of the  $l = 2$  Legendre mode perturbation, we get “lucky” again. We alerted the reader of this possibility in an earlier section. In that case we were able to restore proper behavior by replacing the Godunov algorithm in the radial direction, which has non-differentiabilities at all sonic points, with the previously-described donor cell algorithm, which is non-differentiable only at  $u = 0$  sonic points.

## VII. CONCLUSIONS

We have put forth the hypothesis that a highly desirable condition for the accurate numerical modeling of small per-

turbations imposed on a system of conservation laws is that the numerical time evolution operator satisfy a differentiability condition. The numerical experiments that we present here strongly support that hypothesis. Indeed much of the effort that we have exerted over the past few years in trying to ensure that NRL’s FAST code [3] properly models small-amplitude perturbations has been driven by this design principle. We will be reporting on the results of that effort elsewhere.

However, it must be pointed out here that even if our hypothesized need to satisfy a differentiability condition is correct, the algorithms we have used here to meet that condition, i.e., using a different hydrodynamics algorithm along the shock propagation direction than transverse to it, only address the needs of the ICF pellet implosion problem in the early stages of its evolution, when the fronts are nearly aligned with the transverse direction. As the perturbations enter the fully nonlinear regime, the need for a front-capturing method in the transverse direction will probably arise, pushing us again back in the direction of using non-differentiable algorithms. Our empirical experience in this regime suggests that the situation is not as bleak as it sounds, for we have thus far found differentiability to be far less critical an issue when endeavoring to model the evolution of *large* amplitude perturbations, i.e., perturbations in the nonlinear regime, than small ones. Nonetheless we would prefer not to rely on this experience. Our hope is that the future will bring forth the development of “high resolution” methods satisfying the differentiability condition, as we discussed in the last section, giving us the robustness of the present methods in the presence of fronts, combined with the differentiability we need to properly model the evolution of small perturbations.

- 
- [1] J. D. Lindl, *Inertial Confinement Fusion* (Springer-Verlag, New York, 1998).
  - [2] D. Mihalas and B. Weibel-Mihalas, *Foundations of Radiation Hydrodynamics* (Dover, New York, 1999).
  - [3] J. H. Gardner, A. J. Schmitt, J. P. Dahlburg, C. J. Pawley, S. E. Bodner, S. P. Obenschain, V. Serlin, and Y. Aglitskiy, *Phys. Plasmas* **5**, 1935 (1998).
  - [4] A. J. Schmitt, A. L. Velikovich, J. H. Gardner, C. Pawley, S. P. Obenschain, Y. Aglitskiy, and Y. Chan, *Phys. Plasmas* **8**, 2287 (2001).
  - [5] P. D. Lax and B. Wendroff, *Comm. Pure Appl. Math.* **13**, 217 (1960).
  - [6] J. P. Boris, in *Computing as a Language of Physics* (International Atomic Energy Commission, 1971), pp. 171–189.
  - [7] J. P. Boris and D. L. Book, *J. Comput. Phys.* **11**, 38 (1973).
  - [8] B. van Leer, *J. Comput. Phys.* **32**, 101 (1979).
  - [9] P. Colella and H. M. Glaz, *J. Comput. Phys.* **59**, 264 (1985).
  - [10] P. Colella and P. R. Woodward, *J. Comput. Phys.* **54**, 174 (1984).
  - [11] A. Harten, B. Engquist, S. Osher, and S. R. Chakravarthy, *Journal of Computational Physics* **71**, 231 (1987).
  - [12] G. S. Jiang and C. W. Shu, *J. Comput. Phys.* **126**, 202 (1996).
  - [13] S. Liu and T. Chan, *J. Comput. Phys.* **115**, 200 (1994).
  - [14] A. Harten, *SIAM Journal on Numerical Analysis* **21**, 1 (1984).
  - [15] B. Cockburn and C. W. Shu, *J. Comput. Phys.* **141**, 199 (1998).
  - [16] S. K. Godunov, *Matematicheskii Sbornik* **47**, 271 (1959).
  - [17] R. Richtmyer and K. Morton, *Difference Methods for Initial Value Problems, 2nd ed.* (Interscience, New York, 1967).
  - [18] T. W. Johnson and J. M. Dawson, *Phys. Fluids* **16**, 722 (1973).
  - [19] L. Spitzer, Jr., *Physics of Fully Ionized Gases, 2nd Revised Ed.* (Interscience Publishers, New York, 1962).
  - [20] A. L. Velikovich, J. P. Dahlburg, J. H. Gardner, and R. J. Taylor, *Phys. Plasmas* **5**, 1491 (1998).
  - [21] V. N. Goncharov, *Phys. Rev. Lett.* **82**, 2091 (1999).
  - [22] Y. Aglitskiy, A. L. Velikovich, M. Karasik, V. Serlin, C. J. Pawley, A. J. Schmitt, S. P. Obenschain, A. N. Mostovych, J. H. Gardner, and N. Metzler, pp 9, 2264 (2002).
  - [23] J. Quirk, *Int. J. Numer. Meth. Fluids* **18**, 555 (1994).